Observation of ultrashort pulse propagation anisotropy in a semiconductor quantum nanostructure optical waveguide by cross-correlation frequency resolved optical gating spectroscopy

Noriaki Tsurumachi,[a] Kazunori Hikosaka, Xue-Lun Wang, and Mutsuo Ogura
National Institute of Advanced Industrial Science and Technology (AIST), Central 2, 1-1-1 Umezono, Tsukuba, Ibaraki, 305-8568 Japan, CREST-Japan Science and Technology Corporation (JST), and New Energy and Industrial Technology Development Organization (NEDO), Sunshine 60 Building, 3-1-1 Higashi Ikebukuro, Toshima-ku, Tokyo 170-6028, Japan

Naoki Watanabe and Toshiaki Hattori
Institute of Applied Physics, University of Tsukuba, 1-1-1 Tennodai, Tsukuba, Ibaraki, Japan

(Received 10 March 2003; accepted 11 June 2003)

Femtosecond optical pulse propagation in a quantum well (QW) waveguide and a quantum wire (QWR) waveguide was investigated by cross-correlation frequency resolved optical gating (XFROG) spectroscopy. An optical pulse transmitted through the GaAs QW waveguide was found to stretch greatly from 140 fs to almost 1 ps due to nonlinear dispersion around the heavy hole exciton resonance at transverse electric polarization in a near resonant experiment. In contrast, only slight chirping of the pulse transmitted was observed either at transverse magnetic polarization or off resonance for both polarizations. In the GaAs QWR waveguide, the polarization anisotropy of a crescent shaped QWR could also be observed in terms of dispersion by XFROG spectroscopy in spite of the small absorption compared with that in the QW. © *2003 American Institute of Physics.* [DOI: 10.1063/1.1596368]

I. INTRODUCTION

Semiconductor optical waveguides with quantum wells (QWs), quantum wires (QWRs) or quantum dots (QDs) as a active materials are important components for ultrafast photonic devices such as laser diodes, semiconductor optical amplifiers, and photonic switches. Knowledge of their properties for the transmission of ultrashort optical pulses is essential for optimal design of these devices. However, distortion of optical pulses transmitted through them is very complicated, because both the amplitude and phase are changed by numerous linear optical factors such as refractive index dispersion, absorption or gain, and nonlinear optical effects such as two-photon absorption or self-phase modulation.[1,2] Therefore, transmission properties of the optical waveguide in both time and frequency domains should be fully characterized before designing future photonic devices.

The quantum nanostructure waveguide has been shown to possess anisotropic optical properties which depend strongly on the direction of polarization of the incident light field. Several groups have investigated the anisotropic transmission properties of quantum nanostructure waveguides in the frequency domain using continuous wave (cw)-light sources.[3–5] Weiner *et al.* observed the absorption anisotropy between polarization parallel and perpendicular to the plane of the QW layer in a transmission experiment.[3] Sonek *et al.* investigated the refractive index dispersion anisotropy in QWs by the grating coupling method.[4] In their studies, each optical constant was studied independently. On the other hand, both the absorbance and the refractive index can be obtained at the same time without Kramers–Kronig analysis by Fourier-transform analysis of linear cross-correlation interferograms between the light field input and the light field output from the sample in the time domain technique.[6,7] However, these techniques do not provide the information on the temporal pulse shape including the nonlinear optical effects.

Recently, frequency resolved optical gating (FROG) has often been used for full characterization of ultrashort optical pulses, since it gives information on both the amplitude and phase of the pulse field.[8] Although second harmonic generation (SHG) FROG is one of the most widely used methods for ultrashort pulse characterization,[9] it often fails to retrieve a weak pulse. Cross-correlation FROG (XFROG) is more suitable for characterization of weak pulses than SHG-FROG because the former is based on the sum-frequency signal between a weak test pulse and a strong gate pulse.[10,11] Since the amplitude and the phase of the pulse in the time domain can easily be transformed into the amplitude and phase information in the frequency domain, the XFROG technique can be used to measure a complex transmission coefficient of the sample in the linear regime. Not only the complex transmission coefficient in the frequency domain but also deformation of the ultrashort pulse in the time domain can be observed directly at the same time in both the linear region and the nonlinear region by XFROG spectroscopy.[1,12–14]

In this article, the transmission properties, including the polarization anisotropy of the QW waveguide and of the QWR waveguide, are investigated by XFROG spectroscopy.

[a]Electronic mail: n-tsurumachi@aist.go.jp

II. EXPERIMENT

A. XFROG spectroscopy

In general, the ultrashort optical pulse field can be written in the time domain as

$$E(t)=\mathrm{Re}\{\sqrt{I(t)}\exp[i\omega_0 t-i\varphi(t)]\}, \tag{1}$$

where $I(t)$ and $\varphi(t)$ are intensity of the wave form and temporal phase of the pulse, respectively, and ω_0 is the carrier frequency. The instantaneous pulse frequency $\omega(t)$ can be derived from the temporal phase as

$$\omega(t)=\omega_0-\frac{d\varphi(t)}{dt}. \tag{2}$$

The pulse field can also be written in the frequency domain as

$$\tilde{E}(\omega)=\sqrt{\tilde{I}(\omega-\omega_0)}\exp\{i\tilde{\varphi}(\omega-\omega_0)\}, \tag{3}$$

where $\tilde{E}(\omega)$ is the Fourier transform of $E(t)$. $\tilde{I}(\omega-\omega_0)$ and $\tilde{\varphi}(\omega-\omega_0)$ are the power spectrum and spectral phase, respectively. The group delay $\tilde{t}(\omega-\omega_0)$ can be derived from the spectral phase as

$$\tilde{t}(\omega-\omega_0)=\frac{d\tilde{\varphi}(\omega-\omega_0)}{d\omega}. \tag{4}$$

Both the amplitude of and phase information on the light flied can be obtained by the XFROG method. XFROG spectroscopy is based on an intensity cross-correlation measurement. The electric field of the cross-correlation signal E_{cross} for sum-frequency generation has the following form:

$$E_{\mathrm{cross}}(t,\tau)=E_{\mathrm{gate}}(t)E_{\mathrm{test}}(t-\tau), \tag{5}$$

where E_{gate} and E_{test} are the electric fields of the gated pulse and the test pulse, respectively. The spectrum of cross correlation recorded as a function of delay τ between the test and gated pulses yields a XFROG trace of

$$I_{\mathrm{XFROG}}(\omega,\tau)=\left|\int_{-\infty}^{+\infty}E_{\mathrm{cross}}(t,\tau)\exp(i\omega t)dt\right|^2. \tag{6}$$

The XFROG algorithm based on iterative Fourier transformation with generalized projection is performed to retrieve the unknown test pulse.[10] This algorithm needs input data from both the experimentally obtained XFROG trace $I_{\mathrm{XFROG}}(\omega,\tau)$ and the electric field of the gated pulse $E_{\mathrm{gate}}(t)$, which was previously characterized well by another method, for example, SHG FROG. Staring with an initial guess of the test pulse, the iterative Fourier transform algorithm generates a better guess, which is closer to the correct complex electric field.

The complex transmission properties of a sample can be derived from the amplitude of and phase information on both the input and output light fields. Thus, the XFROG method can be used as a spectroscopic tool for characterization of the optical properties of the sample such as for waveguide structures.

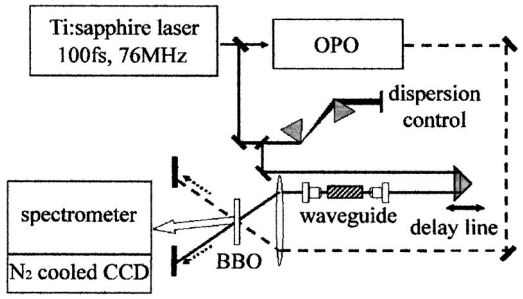

FIG. 1. Schematic of the experimental setup for XFROG spectroscopy.

B. Experimental setup

Figure 1 shows a schematic of the experimental setup in this study. The laser system we used was based on a mode-locked Ti:sapphire laser and an optical parametric oscillator (OPO). The output from the Ti:sapphire laser, whose wavelength and pulse duration were around 800 nm and about 100 fs, respectively, was focused onto a facet of the waveguide by a microscope objective with magnitude of 20 after compensation for chirping using a prism pair. The spot diameter of the incident laser at the waveguide's facet was about 5 μm. Part of the Ti:sapphire laser output was used to pump the OPO. The pulse and the gate pulse transmitted from the OPO, whose wavelength and pulse duration were around 1550 nm and about 150 fs, respectively, overlapped a 0.5 mm thin β-BaB_2O_4 (BBO) crystal and sum-frequency light was generated. The sum-frequency-light spectra were recorded with a liquid N_2 cooled charge coupled device (CCD) camera as a function of the delay between the pulse transmitted and the gate pulse. We refer to them as XFROG traces. By retrieving the phase from an experimentally obtained XFROG trace,[10,11] we obtained both the amplitude and phase of the pulse.

A combination of Ti:sapphire laser and OPO (in a two-color configuration) enables background-free measurement. Since the wavelength of the sum-frequency signal and the SHG signal from each pulse are different, the sum-frequency signal can easily be resolved by a spectrometer.[15]

The waveguide sample was fixed on the cold finger of a high stability transmission-type helium cryostat (Axess Tech) for the low temperature experiment. Drift of the sample position with respect to the support of the cryostat in all dimensions was less than 1 μm over at least a 3 h period. CCD cameras were used to visualize the facet of the waveguide on both the input and output sides.

C. Quantum nanostructure optical waveguide sample

Based on the discussion above, we employed XFROG spectroscopy to obtain the complex transmission properties of a semiconductor optical waveguide with GaAs/AlGaAs QWs and QWRs. The QW sample was a graded index-separate confinement heterostructure (GRIN-SCH) optical waveguide that contained three period $GaAs/Al_{0.2}Ga_{0.8}As$ QWs (10 nm). The cladding layer was $Al_{0.4}Ga_{0.6}As$. The temperature dependence of the photoluminescence (PL) spectrum is shown in Fig. 2. The wavelengths of the PL peaks from the QWs, the impurity, and the GaAs substrate are 760, 818 and 830 nm, respectively at 10 K. At 300 K, only the PL peak from the QWs at 810 nm is observed. We

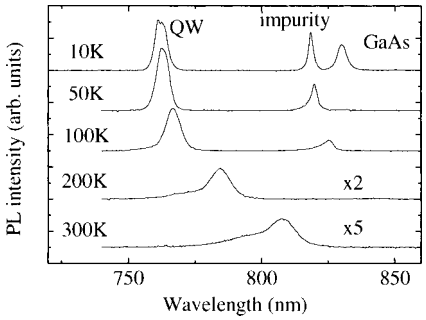

FIG. 2. Temperature dependence of PL spectra on the QW waveguide structure.

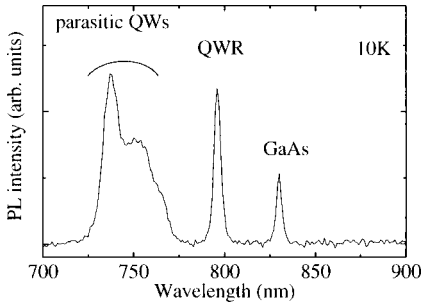

FIG. 4. PL spectrum of the QWR waveguide structure at 11 K.

performed two different XFROG experiments for the QW waveguide. (1) We tuned the input light wavelength to 840 nm, which is off resonance with the exciton transition of the sample kept at 300 K. Here, the length of the waveguide was 700 μm. (2) We tuned the input wavelength to 770 nm, which is near resonance and kept the sample at 10 K. Here, the length of the waveguide was 350 μm.

Figure 3 shows a cross-sectional high resolution scanning electron microscopy (SEM) image of the QWR waveguide sample. The QWR sample was an optical waveguide that contained seven period crescent shaped GaAs/$Al_{0.36}Ga_{0.64}As$ QWRs fabricated by flow rate modulation epitaxy.[16–18] The cladding layer was $Al_{0.63}Ga_{0.37}As$. The flat (001) and the (111)*A* sidewall regions were removed selectively using wet chemical etching, which is effective in suppressing PL from parasitic QWs in the sample.[17] The PL spectrum of the QWR sample at 10 K is shown in Fig. 4. The PL in the QWR is located at 795 nm. The low energy side PL peaks around 750 nm are from residual parasitic QWs and the high energy side PL peak at 830 nm is from the GaAs substrate. In the XFROG experiment for the QWR sample, we tuned the wavelength input to 795 nm, which is resonant with the exciton transition of the QWRs of the sample kept at 10 K. Here, the length of the waveguide was 1000 μm.

III. RESULT AND DISCUSSION

A. Off resonance in the quantum well waveguide

First, the results of the XFROG experiment for off resonance in the QW waveguide as a demonstration of XFROG spectroscopy are described. Figure 5 shows experimentally obtained XFROG traces of pulse input and pulse output of the waveguide in the off resonance experiment. The trace of the pulse output is tilted compared with that of pulse input. This shows that the longer wavelength components travel faster in the waveguide than the shorter wavelength components. The traces of SHG FROG do not show tilting due to ambiguity in the time direction.[8] We obtained both the amplitude and phase of the pulse in the time domain by employing the phase retrieval algorithm.[10,11] The instantaneous frequency of the pulse was calculated from the temporal phase

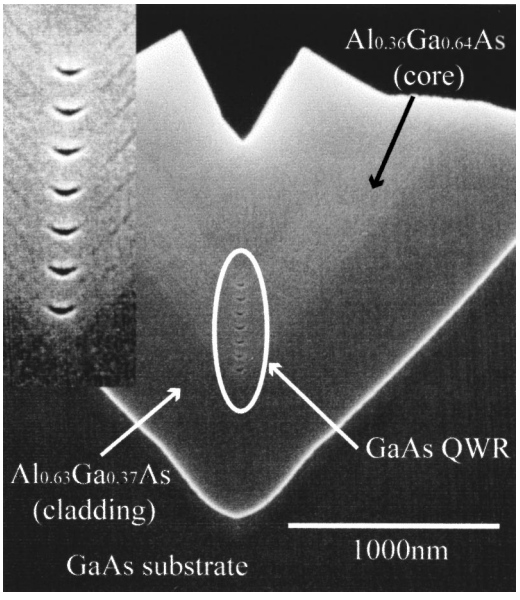

FIG. 3. Cross-sectional SEM image of the QWR waveguide structure.

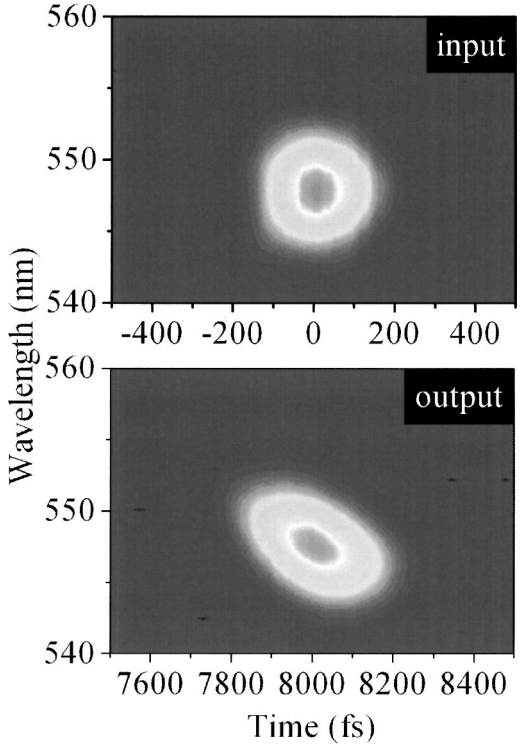

FIG. 5. Experimentally obtained XFROG traces for (a) pulse input and (b) pulse output of the QW waveguide under the off resonance condition.

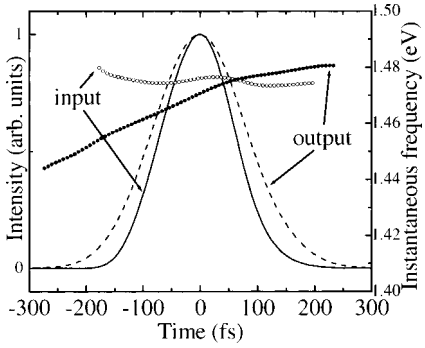

FIG. 6. Intensity and the instantaneous frequency of pulse input and output in the time domain obtained from XFROG traces in the off resonance experiment for the QW waveguide. The solid line is the intensity of the input and the dashed line is that of the output. The open circle is the instantaneous frequency of the input and the closed circle is that of the output.

using Eq. (2). Figure 6 shows the intensity and instantaneous frequency of the pulse obtained in the time domain. The pulse width output is broader than the pulse width input. The instantaneous frequency of the input is almost constant for the whole duration of the pulse, which suggests that the pulse input is almost Fourier transform limited. On the other hand, the instantaneous frequency of the output increases almost linearly from the beginning of the pulse to the end. This clearly shows that the pulse output is linearly chirped due to dispersion of the group velocity of the waveguide in the transparent region. These results show that our XFROG spectroscopy setup can be used for analysis of the propagation properties in waveguide-type semiconductor optical devices.

B. Near resonance in the quantum well waveguide

Next, the results of the XFROG experiment for near resonance in the QW waveguide are described. Figure 7 shows the experimentally obtained XFROG traces for pulse input and pulse output of the waveguide when the input is polarized perpendicular to the QW layer [transverse magnetic (TM) polarization], and the output when the input is polarized parallel to the QW layer [transverse electric (TE) polarization] in the near resonance experiment. For TM polarization, the result is similar to that in off resonance shown in Fig. 5(b). In contrast, with TE polarization, the XFROG trace has a very long tail. Figure 8 shows the intensity and instantaneous frequency of the pulse obtained in the time domain. The instantaneous frequency of pulse input remains almost constant for the whole duration of the pulse as shown in Fig. 8(a). With the TM polarization shown in Fig. 8(b), the instantaneous frequency increases over time, although the oscillating behavior seen suggests the existence of higher-order dispersion. We cannot distinguish between this higher-order dispersion and linear chirp under off resonant conditions solely from the XFROG trace. However, by obtaining the phase, we were able to observe the difference. With the TE polarization shown in Fig. 8(c), the pulse has a very long tail and the instantaneous frequency changes nonlinearly over time. We can also obtain both the amplitude and phase

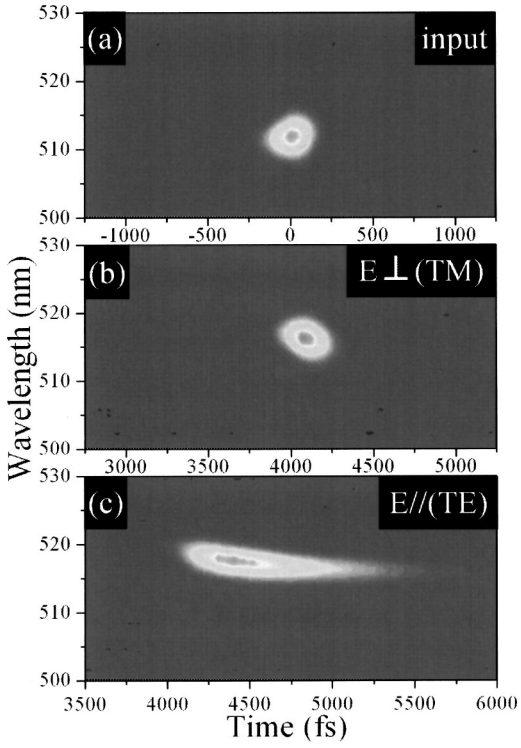

FIG. 7. Experimentally obtained XFROG traces for (a) pulse input, for (b) TM polarization output, and for (c) TE polarization output in the near resonance experiment for the QW waveguide.

of each pulse in the frequency domain. The group delay can be obtained from the spectral phase using Eq. (4).

Figure 9 shows the transmitted intensity and group delay dispersion obtained in the frequency domain. The solid line is the intensity of TE polarization and the dashed line is that

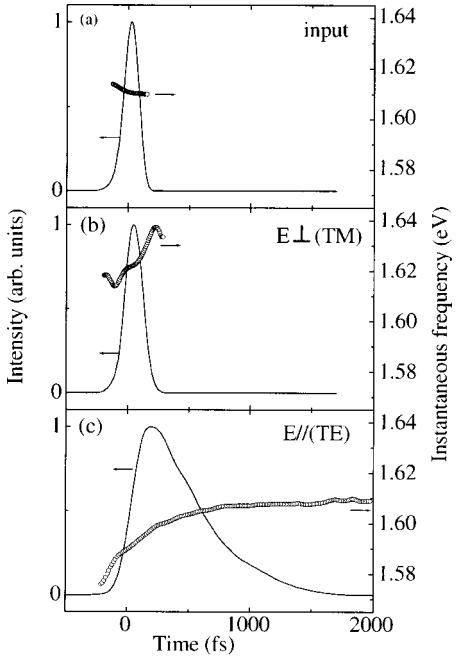

FIG. 8. Intensity and the instantaneous frequency of the pulse in the time domain obtained from XFROG traces for (a) pulse input, for (b) TM polarization pulse output and for (c) TE polarization pulse output in the near resonance experiment for the QW.

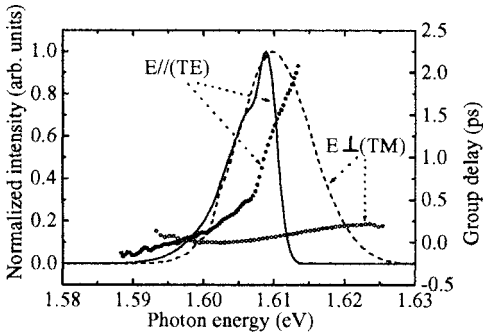

FIG. 9. Intensity and group delay dispersion in the frequency domain obtained from the XFROG trace in the near resonance experiment for the QW waveguide. The solid line is the intensity of TE polarization and the dashed line is that of TM polarization. The closed circle is the group delay of TE polarization and the open circle is that of TM polarization.

of TM polarization. The closed circle is the group delay of TE polarization and the open circle is that of TM polarization. With TE polarization, the intensity of the higher energy side transmitted is greatly reduced and the group delay dispersion bends more than with TM polarization. These differences between TE and TM polarization are attributed to the absorption anisotropy of QWs.[3,4] With TE polarization, QWs have both heavy hole (hh) and light hole (lh) exciton absorption. In contrast, with TM polarization, hh exciton absorption is forbidden by the polarization selection rule so only lh exciton absorption can be observed. The lh exciton absorption peak is located on the higher energy side of the hh exciton absorption peak. Since the center wavelength of pulse input was tuned towards the lower side of the hh exciton absorption peak, TE polarization light was influenced by absorption and dispersion more than TM polarization light. Therefore, the spectrum of the pulse output for TE polarization is deformed and the pulse width is greatly stretched due to nonlinear chirp.

The origin of the ''small step'' on the low energy side in Fig. 9 might be an error in analysis since the intensity of TE polarization transmitted was quite weak compared to TM polarization due to absorption anisotropy. Moreover the spectrum of TE suggests that absorption saturation exists. So it is difficult to discuss the difference in energy between hh and lh transitions just by the spectra of this sample. In order to investigate details of the optical properties of the QW itself, it is necessary to optimize the absorption coefficient, waveguide length and waveguide modes. In this article, we emphasize that the amplitude of and phase information on waveguide-type real optical devices such as the pulse wave form, group delay dispersion, transmitted spectrum etc. can be obtained at the same time by XFROG spectroscopy.

C. Resonance in the quantum wire waveguide

Finally, results of the XFROG experiment for the case of resonance in the QWR waveguide are described. Figures 10(a)–10(c) show the experimentally obtained XFROG traces for pulse input, pulse output from the waveguide when the polarization of light was vertical to the direction of confinement of the QWR (TM-like polarization), and output when the polarization of light was in the direction of lateral

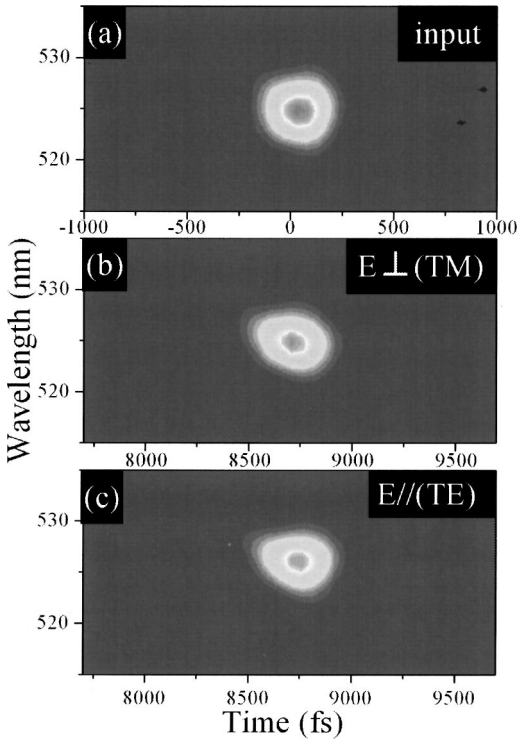

FIG. 10. Experimentally obtained XFROG traces for (a) pulse input, for (b) TM polarization output, and for (c) TE polarization output in the resonance experiment of the QWR waveguide.

confinement of the QWR (TE-like polarization). For both polarizations, the results were not completely the same like, for example, the position of the top of the contour, however, it is quite similar and it is difficult to distinguish one from the other in the XFROG traces. This is because the active volume of the QWR, that is, the influence of absorption during propagation, is much smaller than that of the QW waveguide. Moreover, since there are higher-order waveguide modes in the V-groove waveguide which do not overlap the QWRs, the influence of the absorption of QWRs tends to be smaller. The fact that the XFROG trace shows a single peak suggests that the light of all modes transmitted from the waveguide arrived at the same time on the BBO crystal in this experiment. We cannot distinguish the propagation of each mode even if their refractive indices are different. Since the XFROG trace contains both fundamental mode, which was influenced by absorption, and transparent higher-order mode, the influence of absorption decreased when the component of the higher-order mode increased.

However, we could observe the polarization anisotropy of the QWR waveguide by retrieving the phase. Figure 11 shows the normalized transmitted intensity and group delay dispersion retrieved in the frequency domain. The intensity spectrum of the TM polarization transmitted is almost same as that in the input light spectrum. On the other hand, the peak of the light output spectrum of the TE polarization is redshifted compared with that of the input and the TM polarization due to small absorption on higher-energy side. The group delay dispersion of the TM polarization is almost straight. However, that of the TE polarization bends a little bit, which reflects an anomalous dispersion related to absorp-

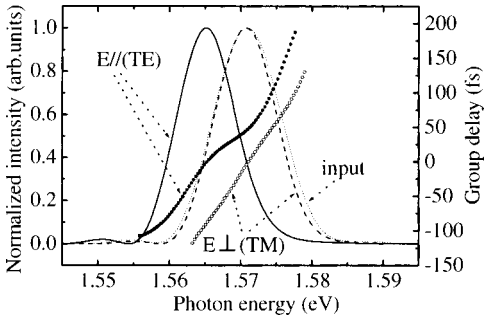

FIG. 11. Intensity and group delay dispersion in the frequency domain obtained from the XFROG trace in the resonance experiment for the QWR waveguide. The solid line is the intensity of TE polarization and the dashed line is that of TM polarization. The dotted line is that of the input. The closed circle is the group delay of TE polarization and the open circle is that of TM polarization.

tion. These differences between TE and TM polarizations are attributed to the absorption anisotropy of the QWRs. The polarization anisotropy has been shown to depend strongly on the cross-sectional shape of the QWR. Martinet *et al*. discussed the absorption anisotropy between TE and TM polarization in a crescent shaped QWR waveguide.[5] They found a genuine QWR transition in TM polarization, e1h2, which originates both from valence band mixing at $k=0$ and from the breaking of symmetry at the heterostructure level, despite mirror symmetry. In TM polarization, the e1h1 transition has no visible feature and the e1h2 transition is fundamental and is located at the higher energy side of the e1h1 transition. Our results also suggest that the absorption edge in the TM polarization is at higher energy compared with that in TE polarization. Although it is difficult to discuss details of the absorption spectrum profile because of small absorption, we also could observe the polarization anisotropy of QWR absorption when light was inserted along the QWR.

In the case of conventional cw absorption spectroscopy of waveguide structures, it is necessary to separate the light transmitted through the waveguide spatially from stray light, which does not enter the waveguide core region due to loss of focus or misalignment, so measurement of the absorption spectrum was comparatively difficult. On the other hand, in this XFROG case, these two different components are easily separated by a time resolved measurement since the arrival of light transmitted through the optical waveguide to the BBO crystal is delayed. For measuring dispersion XFROG spectroscopy has an advantage because it is not necessary to add special structures such as a grating.[4] In this XFROG spectroscopy, both the amplitude and phase information can be obtained at the same time. In order to evaluate details of the optical properties of the QWR, it is necessary to optimize the absorption coefficient, waveguide length, waveguide modes and coupling constant of the waveguide. Here, we point out, however, that the anisotropy of dispersion in the QWR optical device could be clearly observed by this XFROG spectroscopy even for small QWR absorption.

IV. CONCLUSION

We investigated the femtosecond pulse propagation effects in a semiconductor QW waveguide and a QWR waveguide by XFROG spectroscopy. In an off resonance experiment for the QW waveguide, we clearly observed linear chirping of the transmitted pulse. In a near resonance experiment for the QW waveguide, the optical pulse transmitted through the waveguide was found to be stretched greatly from its original duration of 140 fs to almost 1 ps due to nonlinear dispersion around the heavy hole exciton resonance at TE polarization. In contrast, only slight chirping of the transmitted pulse was observed at TM polarization. In the QWR waveguide, the polarization anisotropy of the QWR could be observed by XFROG spectroscopy in spite of the small absorption. The polarization anisotropy of the QW and the QWR retrieved from the XFROG traces was clearly observed in the absorption and the dispersion. XFROG spectroscopy was shown to be a very simple valuable technique for the characterization of waveguide-type semiconductor photonic devices, since transmission properties such as the pulse shape, chirping, absorption and dispersion spectra can easily be obtained at the same time using this technique.

[1] F. Romstad, P. Borri, W. Langbein, J. Mørk, and J. M. Hvam, IEEE Photonics Technol. Lett. **12**, 1674 (2000).
[2] N. Bélanger, A. Villeneuve, and J. S. Aitchison, J. Opt. Soc. Am. B **14**, 3003 (1997).
[3] J. S. Weiner, D. S. Chemla, D. A. B. Miller, A. C. Gossard, W. Wiegmann, and C. A. Burrus, Appl. Phys. Lett. **47**, 664 (1985).
[4] G. J. Sonek, J. M. Ballantyne, Y. J. Chen, G. M. Carter, S. W. Brown, E. S. Koteles, and J. P. Salerno, IEEE J. Quantum Electron. **22**, 1015 (1986).
[5] E. Martinet, M.-A. Dupertuis, L. Sirigu, D. Y. Oberli, A. Rudra, K. Leifer, and E. Kapon, Phys. Status Solidi A **178**, 233 (2000).
[6] K. Naganuma, K. Mogi, and H. Yamada, Opt. Lett. **15**, 393 (1990).
[7] N. Tsurumachi, T. Fuji, S. Kawato, T. Hattori, and H. Nakatsuka, Opt. Lett. **19**, 1867 (1994).
[8] R. Trebino, K. W. Delong, D. N. Fittinghoff, J. N. Sweetser, M. A. Krumbügel, B. A. Richman, and D. J. Kane, Rev. Sci. Instrum. **68**, 3277 (1997).
[9] A. Baltuška, M. S. Pshenichnikov, and D. Wiersma, Opt. Lett. **23**, 1474 (1998).
[10] S. Linden, H. Giessen, and J. Kuhl, Phys. Status Solidi B **206**, 119 (1998).
[11] S. Linden, J. Kuhl, and H. Giessen, Opt. Lett. **24**, 569 (1999).
[12] Y. Mitsumori, R. Kawahara, T. Kuroda, and F. Minami, J. Lumin. **94–95**, 645 (2001).
[13] A. Yabushita, T. Fuji, and T. Kobayashi, Opt. Commun. **198**, 227 (2001).
[14] N. Nishizawa and T. Goto, Opt. Express **8**, 328 (2001).
[15] S. Haacke, R. A. Taylor, I. Bar-Joseph, M. J. S. P. Brasil, M. Hartig, and B. Deveaud, J. Opt. Soc. Am. B **15**, 1410 (1998).
[16] X. L. Wang, M. Ogura, and H. Matsuhata, Appl. Phys. Lett. **66**, 1506 (1995).
[17] X. L. Wang, M. Ogura, and H. Matsuhata, Appl. Phys. Lett. **67**, 804 (1995).
[18] X. Q. Liu, X. L. Wang, and M. Ogura, Appl. Phys. Lett. **79**, 1622 (2001).